1984A&A...138...85F

Astron. Astrophys. 138, 85–92 (1984)

ASTRONOMY
AND
ASTROPHYSICS

The Coma/A 1367 filament of galaxies

P. Fontanelli

Istituto di Astronomia, Universita' di Firenze, Largo E. Fermi 5, I-50125 Firenze, Italy

Received February 9, accepted March 7, 1984

Summary. In the Coma/A 1367 supercluster the surface distribution of galaxies from Zwicky and UGC catalogs outlines a filamentary structure in which the Coma cluster itself is embedded. In its densest part the filament extends for approximately 3.5 h in right ascension and shows an average density contrast of about 2.7 with respect to the nearby regions. The position angle of Coma is well oriented along the filament and points significantly toward another cluster of the filament which also shows an elongated shape in the same direction. A sample of new 21-cm redshifts is used together with the redshifts data available in the literature to study the structure of the filament: the majority of the galaxies on it falls in the velocity range of Coma indicating that the filament is a coherent structure in the three-dimensional space and represents an important element of the supercluster. The possibility that the filamentary structure continues at a lower density contrast to bridge the Lynx-Ursa Major and the Hercules supercluster is discussed.

Key words: galaxies – superclusters – filaments

I. Introduction

The largest hierarchical units of the distribution of matter in the Universe, called second order clusters or superclusters, were initially described as spheroidal aggregates of galaxies separated from each other (Abell, 1961). Although the definition of a supercluster is still at present very qualitative, the initial picture has proved to be inconsistent with that emerging from surveys of redshifts done in several supercluster structures. Today it is widely believed that superclusters are flat asymmetric structures whose principal elements are represented by chains of galaxies and clusters of galaxies in association with large and relatively empty regions of space (Jôeveer et al., 1978). With typical but still uncertain sizes of the order of 50–100 Mpc, superclusters are not to be considered bound units but massive aggregates that participate in the general expansion due to the Hubble flow. Among the many uncertain parameters, a rather well established observational property of superclusters is the lack of symmetry exhibited by these structures and more generally the very clumpy and filamentary way in which galaxies are distributed. As a matter of fact the examination of the two dimensional distribution of nearby galaxies, projected on the celestial sphere, shows several cases of linearly extended features characterized by a shape closely resembling a filament. The most famous example is the Perseus chain, a narrow and dense structure that appears to extend for more than four hours in right ascension and from which several secondary filaments seem to depart: Einasto et al. (1980) have shown that all the galaxies in the chain lie in a strip 4° wide, along which numerous condensations of different richness can be found.

The addition of velocity as a third dimension to the projected distribution of galaxies provides essential informations to the studies of superclustering. In fact, even if the average surface density of galaxies in such filaments is significantly higher than in the surrounding regions, the identification of these structures as real three dimensional units is possible only after a careful analysis of their velocity distribution. In the case of the Hercules group and the group of A 2197–2199, for example, Abell suggested as early as 1961 that they might be connected by a bridge of galaxies and be part of the same supercluster; but only recently Chincarini et al. (1981) were able to show that the bridge exists in velocity space, confirming Abell's hypothesis.

Rich chains of galaxies, like Perseus, in which dense clusters are also embedded are rare; from observations, however, there is evidence of other filamentary structures with a relatively lower density of galaxies. Lucey et al. (1983), for example, have studied the Horologium-Reticulum supercluster showing that between the two main component clusters there is an enhancement of galaxies linearly extended to form a bridge. Giovanelli and Haynes (1982) have described a filamentary structure in the region of the Lynx-Ursa Major. This filament, although located at a lower redshift (4000–5300 km s^{-1}), presents as we will discuss in Sects. II and V positional and morphological similarities to the one that we describe in this paper, which is located in the Coma/A 1367 supercluster ($v \sim 7000$ km s^{-1}).

Due to the presence of the two main concentrations that form the Coma/A 1367 supercluster, observers have preferentially devoted their attention to the regions around and in between the two main clusters. Gregory and Thompson (1978), hereafter GT, have shown the existence in the three dimensional space of a significant population of galaxies linking the two clusters; however relatively little attention has been devoted to other areas of this supercluster, especially for declinations north of Coma where the filamentary structure we are going to discuss is mainly located.

In Sect. II we analyze the surface density distribution of galaxies using a merged version of the CGCG (Zwicky et al., 1961–1968) and UGC (Nilson, 1973) catalogs. In Sect. III we present the data derived from our observations that are used in Sect. IV to study the distribution of redshifts which indicates the coherent nature of the filament. Section V is a discussion of cluster orientations in this filament and of the possibility that its

© European Southern Observatory • Provided by the NASA Astrophysics Data System

1984A&A...138...85F

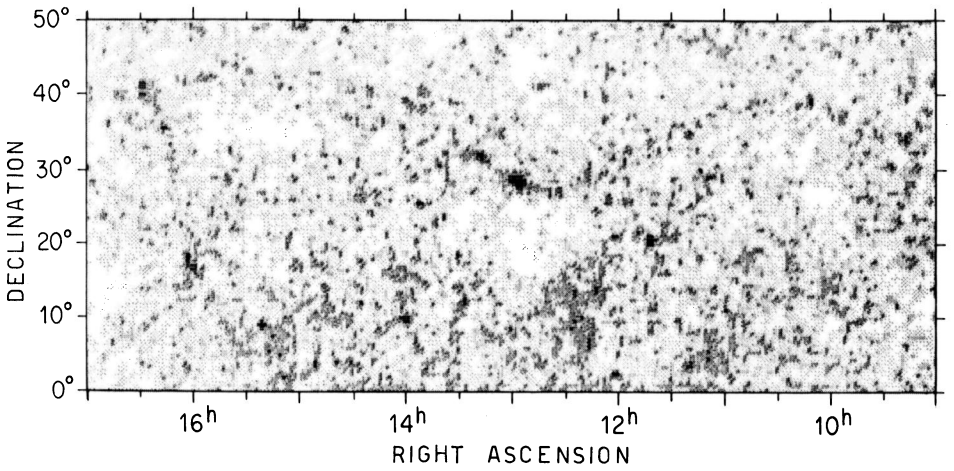

Fig. 1. Shade plot showing the density of galaxies from the CGCG+UGC sample: shade intensity is proportional to the logarithm of the galaxian density averaged over square cells of half a degree on a side. A filamentary enhancement is visible between 10^h40^m and 14^h00^m within the declination range 26°–39°

extensions continue toward the domain of the Hercules supercluster on one side and of the Lynx-Ursa Major on the other. Our conclusions follow.

II. Two-dimensional distribution of galaxies

a) Discussion

The projected distribution of galaxies has been visualized in a great variety of ways on the basis either of catalogs or of counts of galaxy images. The survey done by Shane and Wirtanen (1967) is so far the most complete and deep representation of galaxy distribution available but, because of its depth (it has an apparent limiting magnitude of +18.8), it is not the most appropriate sample to visualize nearby structures that appear smeared out by background objects. Galaxies belonging to nearby superclusters ($v \lesssim 10{,}000\ \mathrm{km\ s^{-1}}$) are in fact expected to lie in a smaller and relatively brighter range of apparent magnitudes compared to that of the Shane and Wirtanen sample. For a supercluster located at a distance $D = v/H$ we can compute the expected range of apparent magnitudes proceeding as follows. Let us assume that $\Phi(M)dM$ represents the galaxian luminosity function and M^* the characteristic absolute magnitude at which $\Phi(M)$ exhibits a rapid change in slope. If $\Phi(M)$ is the same in the region of the supercluster as in less dense areas, then the distribution of apparent magnitudes in the direction of the supercluster should reveal the presence of an increased space density of galaxies with an excess of objects having magnitudes around the value $m = M^* + 5\log(v/H) + 25$ where v is expressed in $\mathrm{km\ s^{-1}}$ and H in $\mathrm{km\ s^{-1}\ Mpc^{-1}}$. For velocities in the range 5000–10,000 $\mathrm{km\ s^{-1}}$ we obtain apparent magnitudes in the range 14.4 – 15.9 ($H = 50\ \mathrm{km\ s^{-1}\ Mpc^{-1}}$, $M^* = -20.6$). Therefore nearby structures can be better investigated using a less deep sample than that of Shane and Wirtanen. We decided to represent the surface distribution of galaxies in the form of a cartesian shade plot (Fig. 1) in which the shade intensity is proportional to the logarithm of the galaxian density averaged over square cells of half a degree by half a degree. This representation appears to be easier to interpret than a contour map. To generate the shade plot we used a merged version of the CGCG and UGC catalogs. While the CGCG contains all the galaxies north of $\delta = -3°$ up to an apparent limiting magnitude of 15.7, the UGC gives more detailed informations on all the galaxies north of $\delta = -2°$ up to an apparent limiting magnitude of 14.5 and also of fainter galaxies having an angular diameter of at least one minute of arc. Therefore a merged version of the two catalogs combines the CGCG completeness at 15.5 with the fainter galaxies reported only in the UGC. In the process of merging particular care has been devoted to the rejection of common objects that may possess slightly differing coordinates in the two catalogs. Visual inspections of Palomar Sky Survey prints have been made in selected areas to test our merging algorithm.

Figure 1 represents the surface distribution of galaxies in a large area of sky where at least three major superclusters are known to be present: Virgo, Coma/A 1367 and Hercules. The clusters Coma and A 1367 appear as the darkest spots located respectively at 12^h57^m, +28° and at 11^h42^m, +20°, while the extended density enhancement visible around 12^h20^m, +10° corresponds to the Virgo area. The clusters forming the Hercules group can be spotted around 16^h, +18°. Many other clusters and groups of galaxies can be easily identified in the shade plot (see for example A 2197 and A 2199 around 16^h26^m, +40°). The inspection of Fig. 1 reveals the presence of a long filamentary structure embedding the Coma cluster as well as other Zwicky clusters (Zwicky et al., 1961–1968) of distance class "near" (Table 1). The most relevant part of the filament is extending linearly from 10^h40^m, +39° toward the south-east; around 12^h40^m, +27° the structure begins to turn north, engulfing the Coma cluster and continuing again linearly up to 14^h00^m, +39°. The two sections of the filament can be fitted respectively with the equations:

$$\delta = -6.0\alpha + 103 \quad \text{between } 10^h40^m \text{ and } 12^h40^m, \tag{1}$$

$$\delta = 10.3\alpha - 105 \quad \text{between } 12^h50^m \text{ and } 14^h00^m, \tag{2}$$

where δ and α are the coordinates of the filament axis expressed respectively in degrees and hours.

On both ends of this more conspicuous section, the eye seems to follow the filament although at a much weaker density level: on the east side forming a large arc ending in correspondance of the clusters A 2197–2199 around 16^h, +40°; on the west side bifurcating in two branches: one leading north pointing toward the Lynx-Ursa major filament (Giovanelli and Haynes, 1982) (the beginning of this structure is visible in Fig. 1 around 9^h30^m, +49°) and the other turning south in direction of A 779 (9^h11^m, +34°). A 1185 (11^h05^m, +29°) seems also to be connected to the Coma filament by a weak chain of clusters, roughly one hour long, departing from the main axis of the filament around 12^h15^m, +28°. Another important feature of the distribution of galaxies, clearly evident

© European Southern Observatory • Provided by the NASA Astrophysics Data System

1984A&A...138...85F

Table 1. "Near" Zwicky clusters

Cluster	RA (1950)	Dec (1950)	ZW type
ZW 184−24	$10^h42^m.4$	39°10′	MC
ZW 185−61	$10^h57^m.2$	38°04′	Open
ZW 185−62	$11^h07^m.7$	36°10′	Open
ZW 185−24	$11^h09^m.1$	38°06′	Compact
ZW 185−27	$11^h17^m.6$	33°52′	Open
ZW 185−26	$11^h23^m.9$	35°41′	Open
ZW 185−29	$11^h26^m.4$	36°56′	MC
ZW 185−41	$11^h30^m.9$	34°35′	Open
ZW 186−37	$11^h42^m.2$	34°56′	MC
ZW 157−17	$11^h55^m.0$	31°27′	MC
ZW 187−32	$12^h04^m.7$	33°19′	Open
ZW 158−16	$12^h17^m.5$	29°15′	MC
ZW 158−15	$12^h24^m.6$	31°31′	MC
ZW 160−1	$12^h57^m.1$	28°06′	Compact
ZW 160−7	$13^h19^m.6$	31°35′	Open
ZW 190−21	$13^h26^m.6$	37°50′	MC
ZW 190−10	$13^h52^m.9$	38°56′	MC

from Fig. 1, is the presence, at the limiting magnitude of our sample, of large voids (the largest two are located around 12^h45^m, +21 and 15^h30^m, +35°) i.e. of regions that seem to contain no rich clusters and only a small number of bright galaxies.

The above description is indeed qualitative and somewhat subjective. Nevertheless the visual impression given by the shade plot reproduces the distribution and the richness of Zwicky clusters in the region that have been recognized to be the principal tracers of supercluster structures (Einasto et al., 1980): used together with velocity informations, they can be an useful guide to find the true distribution of matter in superclusters. Finally it should be stressed here that this qualitative picture is in good agreement with the adiabatic scenario and its predicted cellular structure (Doroshkevich et al., 1978 and references therein), according to which practically all clusters are located in filaments, so that most of the matter is concentrated in strings that fill only a very small fraction of the total volume of the Universe. We will return to this point in Sect. V.

b) Density contrast in the filament

We have computed the average surface density contrast in the portion of the filament described by Eqs. (1) and (2) counting the number of galaxies in our merged CGCG+UGC sample along north-south strips across the filament, each strip being divided in circular fields of 1° radius separated 30′ in declination from each

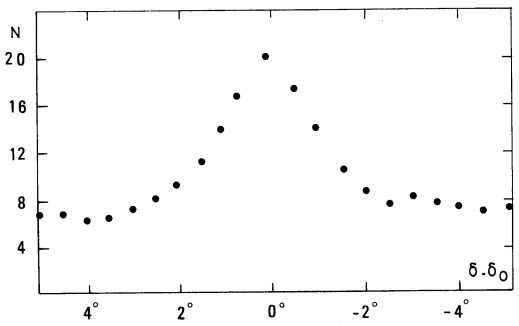

Fig. 2. Average density profile along the filament: the surface density contrast is on average a factor 2.7 with respect to the nearby regions and shows an uncorrected width of about 2.0°

other. The strips are equally spaced every 10^m in right ascension. An area of 2° radius has been excluded from the counts around Coma, which is the richest cluster embedded in the filament. We have accumulated the counts made in different strips according to Eqs. (1) and (2), obtaining the average density profile of the filament (Fig. 2). We have verified that the obtained profile is substantially independent from the positions of the strips and the type of sampling we have used. The average density contrast in the filament is about a factor 2.7 with respect to the nearby regions. The average width of the profile at half peak intensity is about 2°, which gives an average width perpendicular to the filament axis of 1°.7. Even if we exclude from the counts the area of the cluster ZW 160-7, which is after Coma the densest in the filament, the density contrast does not drop below 2.6 indicating that, as far as the projected density of galaxies is concerned, the filament is indeed a significant enhancement of the distribution of galaxies in this region of sky.

It is well known that at low galactic latitudes the distribution of galaxies is severely affected by the presence of gas and obscuring clouds near the plane of our Galaxy. The area of sky in which the filament lies is all at fairly high galactic latitude, so its seems reasonable to expect that galactic extinction does not substantially alter the appearance of the filament. To verify this assumption, we have generated a map of galactic extinction (Fig. 3) from column density of galactic H I and Shane-Wirtanen counts of galaxies according to the formulas given by Burnstein and Heiles (1978). The region is divided into cells of 1 square degree and each cell is filled according to its galactic extinction which ranges from less than 0.01 mag (empty cells) to about 0.17 mag (completely filled cells). The inspection of Fig. 3 shows that in the large region of sky in which the filament is located extinction is typically lower than

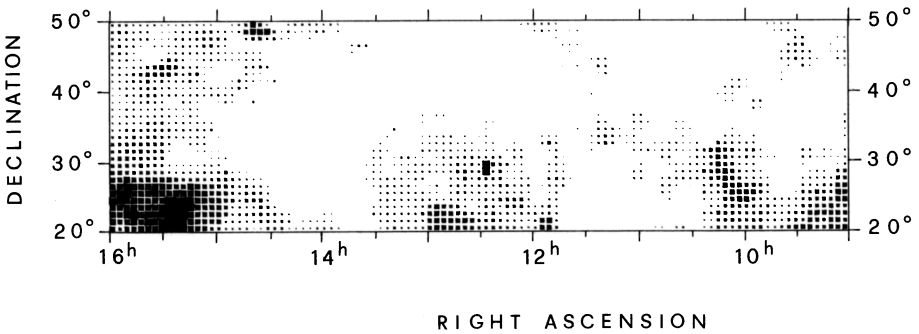

Fig. 3. Map of galactic extinction computed from column density of galactic H I and Shane-Wirtanen counts of galaxies as described in Burstein and Heiles (1978). In the region of the sky where the filament is located extinction is typically lower than 0.01 mag and can be neglected in the density computation

© European Southern Observatory • Provided by the NASA Astrophysics Data System

1984A&A...138...85F

Table 2. Parameters of detected galaxies

UGC	NGC or IC	R.A. h m s	Dec. ° ′ ″	Type	m_z	Size (arc min)		$v_\odot$ (km s^{-1})	W (km s^{-1})	$\int Sdv$ (Jy-km s^{-1})	rms (mJy)
(1)	(2)	(3)	(4)	(5)	(6)	(7)		(8)	(9)	(10)	(11)
6152		11 3 23.1	30 12 20	SBB	15.3	1.30	0.50	8932	419	1.95	1.06
6314		11 15 30.7	30 40 6	S..	15.1	1.00	0.70	7880	334	2.76	1.25
6507		11 28 37.2	34 28 53	SBC	15.6	1.50	1.00	6309	258	5.65	2.55
6539		11 30 44.6	32 52 47	SB-C	15.4	1.50	0.30	6260	347	4.75	2.83
6783		11 46 21.6	31 35 0	DW-IRR	17.0	1.10	0.80	6507	163	2.63	2.32
6872	I2973	11 51 15.5	33 38 35	SBC	14.5	1.50	0.80	3208	210	6.19	2.46
6905		11 53 11.5	30 13 13	SB	16.0	1.10	0.50	6785	391	2.43	1.21
6915	I2978	11 53 48.0	32 17 53	SC	15.4	1.10	0.50	3189	315	2.23	0.95
6932		11 54 53.7	31 21 47	IRR	15.5	1.10	0.40	6882	172	2.40	2.09
6943	N3984	11 55 16.0	29 19 16	SBB	14.8	1.20	1.10	6408	86	3.21	1.71
6968		11 56 9.5	28 34 7	S..	15.2	3.00	1.00	8232	543	7.04	1.25
6981	I2985	11 56 38.1	31 0 40	SB..	15.2	1.10	0.60	3322	160	2.32	1.02
6987		11 56 57.4	30 26 10	SBB	15.3	1.30	0.70	8775	357	2.52	1.27
7012		11 59 28.9	30 7 40	SC	14.3	2.10	1.10	3079	223	9.52	2.02
7017		11 59 49.1	30 8 20	SB	14.4	1.90	0.40	3149	344	7.08	1.35
7031		12 0 48.0	29 41 50	SB-C	15.2	1.70	0.25	3568	265	4.86	1.29
7217		12 10 28.5	25 33 33	S..	15.6	1.70	0.20	7301	354	4.67	2.12
7302		12 14 17.5	30 32 53	DW	17.0	1.00	0.10	3836	93	3.84	2.74
7374		12 17 13.5	29 8 23	S..	15.3	1.10	0.70	7634	355	1.56	0.95
7419	I3203	12 19 14.5	26 9 46	SB	15.7	1.50	0.20	6928	598	4.63	1.94
7495	I3300	12 22 34.0	26 14 7	SC:	15.3	1.10	0.25	6671	404	1.88	1.06
7597		12 25 57.4	28 57 7	S..	16.0	1.30	0.50	4462	216	4.44	1.51
7616	I3402	12 26 29.5	29 8 20	SB-C	15.7	1.00	0.15	8019	516	2.77	0.99
7670	I3454	12 29 9.5	27 46 20	SB:	15.7	1.30	0.20	7009	366	2.01	0.77
7724	I3516	12 31 48.6	27 45 40	SB-C	16.0	1.30	0.15	6858	370	3.47	1.61
7750		12 32 35.5	30 1 13	S..	15.1	1.40	0.50	8047	477	3.37	1.56
7787	I3587	12 34 20.0	27 49 27	SC	16.0	1.40	0.15	7331	406	5.51	1.89
7789	I3592	12 34 25.3	28 8 10	SA?	15.3	1.30	0.40	7511	376	3.38	1.67
7877		12 40 19.6	27 32 50	S..	16.5	1.20	0.20	5909	360	2.63	1.14
7891		12 40 37.3	30 59 33	DBLSYS	15.5	1.00	0.50	7182	194	2.16	1.17
7955		12 44 44.5	26 59 14	SC	16.0	1.40	0.20	6761	422	1.88	0.97
7981		12 47 15.6	31 1 34	SC	16.0	1.10	0.15	4844	250	2.35	1.68
8004		12 49 13.3	31 37 27	SC	15.1	1.90	0.60	6187	313	4.45	2.43
8294		13 10 36.5	31 31 27	SC	15.2	1.00	0.80	6073	231	2.56	1.67
8346		13 14 21.3	31 38 53	SB..	16.0	1.10	0.50	5771	235	1.75	1.28
8359		13 15 18.4	27 49 7	SA-B	15.0	1.60	0.60	6994	396	2.02	0.94
8363		13 16 24.0	27 59 40	IRR	15.6	1.30	0.90	2458	155	5.59	1.96
8392		13 18 53.5	31 29 0	SC	15.3	1.60	1.00	5081	204	4.74	1.41
8418		13 21 23.5	30 49 27	SC	16.5	1.10	0.10	7016	379	3.68	1.21
8496		13 27 58.4	31 35 27	MULSYS	14.9	1.30	0.70	4827	268	7.03	0.98
8497		13 28 7.0	30 17 13	S..	15.1	1.10	0.70	11177	496	3.78	0.92
8510		13 28 58.6	29 37 30	SB-C	15.6	1.20	1.10	14368	185	2.21	1.08
8517		13 29 37.8	31 17 27	S..	16.0	1.00	0.40	4655	204	2.78	1.24
8539		13 31 12.6	33 17 55	S..	14.4	1.40	0.50	7353	414	5.41	1.37
8548		13 31 57.0	31 40 53	SB?..	15.5	1.30	0.60	5017	204	6.32	2.23
8560		13 32 38.1	31 39 0	SB	15.1	1.30	1.00	4962	229	10.64	1.72
8605		13 34 37.8	32 21 0	DW SP	18.0	1.80	0.80	3006	97	3.78	1.98
8608		13 34 43.5	32 1 20	SC	15.7	1.40	0.15	3006	218	4.63	2.22
8609		13 34 43.3	33 49 27	SC/SBC	16.0	1.10	0.90	7758	247	3.45	1.77
8636		13 36 52.4	29 12 46	SB:C	15.4	1.00	0.90	9749	215	2.32	1.83
8879		13 55 21.3	26 0 54	SC	15.7	1.60	0.25	8596	496	3.62	1.16
8911		13 57 23.6	28 18 13	SC	15.3	1.20	0.80	10940	305	2.77	0.79

0.01 mag. Average extinction values of about 0.10 and 0.05 mag are present respectively around 15^h30^m, $+43°$, where the Coma filament seems to merge into the Hercules supercluster, and in the west outskirts of Coma. Figure 3 confirms that the distribution of galaxies in this region of sky is not altered by the presence of our Galaxy and that the counts we have made in order to find the average density contrast in the filament do not need to be corrected for extinction.

III. Observational data

a) Equipment and observing procedures

All 21-cm line observations described in this paper were made in June-July 1981 using the 305 m telescope of the Arecibo observatory[1]. At any time part of the reflecting surface was illuminated by a 14-m dual polarization feed, simultaneously collecting two independent circularly polarized components of the incoming signal. These were successively amplified by a dual channel GaAsFet receiver which typically gave system temperatures in the range 45–60 K. The spectral characteristics of the signal were analyzed into a 1008-channel autocorrelation spectrometer operating in a four quadrant mode of 252 channels each. Because none of the redshifts of the observed galaxies was previously known, each quadrant in the autocorrelator was offset from the next by 7.5 MHz to cover a total bandwidth of 32.5 MHz, corresponding to about 7100 km s^{-1} at the redshift of Coma. If the emission feature of a galaxy detected in this "search" mode did not show a good signal to noise ratio, we observed it again with a different configuration of the autocorrelator in which the four quadrants were covering the same frequency range. In this case the final profile of the galaxy was obtained combining with the proper weight spectra taken in different observing modes. As the zenith angle exceeds 10°, the antenna response degrades and for a zenith angle of 20° the sensitivity to a point source has decreased about 60% of its initial value (zenith angle less than 10°). As a function of frequency the gain drops with a roughly parabolic behaviour, characterized by a 3 dB bandwith of about 45 MHz, from the peak frequency. This maximum frequency response of the feed can be shifted by a few tens of MHz by raising or lowering the feed itself. Corrections for zenith angle and frequency dependence were applied to all spectra. Calibrations for the flux density scale were frequently obtained in the course of the observing run using continuum sources from the catalog of Bridle et al. (1972). The observations were carried out in a total power mode in which 5-min long ON-source scans were followed by OFF-source scans of the same duration and done with the same telescope configuration as the ON.

b) The data

Because we will reobserve some of the non-detected galaxies on a different velocity range and we are planning to expand our redshift sample in this area of the sky and at higher declinations, we present here only a list (Table 2) of the galaxies detected during this

1 The Arecibo Observatory is part of the National Astronomy and Ionosphere Center, which is operated by Cornell University under contract from the National science Foundation

© European Southern Observatory • Provided by the NASA Astrophysics Data System

1984A&A...138...85F

program: all of them are spirals selected from the UGC catalog. The list of the non-detected galaxies will be given elsewhere (Fontanelli et al., in preparation) together with a discussion of the H I and integral properties of the filament galaxies. The entries of Table 2 are as follows:

Column (1): Source number of the galaxy taken from the UGC.
Column (2): NGC or IC designation.
Columns (3) and (4): 1950 coordinates measured on the Palomar Observatory Sky Survey (POSS) prints with an overlay technique similar to that of Dressel and Condon (1976).
Column (5): Morphological type taken from the UGC.
Column (6): Apparent blue photographic magnitude from the CGCG if lower than 15.7, otherwise adopted from the UGC.
Column (7): Major and minor diameter in decimal arcminutes adopted from the UGC.
Column (8): Heliocentric radial velocity ($km\,s^{-1}$) based on 21-cm line observations defined as the average between the values obtained by computing the width at 50% of the mean and at 20% of the peak flux.
Column (9): H I profile width ($km\,s^{-1}$) defined as the average between the values measured at 50% of the mean and at 20% of the peak flux.
Column (10): Area under the H I profile, expressed in $Jy\,km\,s^{-1}$.
Column (11): rms noise figure of the spectrum computed in the region not containing the H I feature.

Line profiles of the galaxies listed in Table 2 are shown in Fig. 4: velocity scales are heliocentric; the number in the upper left corner of each profile represents the flux density scale range between tick marks of that spectrum. All profiles were smoothed by convolution with a rectangular function three channels wide and later with an Hanning cosine function. The profiles are shown before baseline removal and the smooth polynomial curve superimposed represents the baseline we have subtracted before computing the parameters of the line.

The galaxies UGC 6783 and UGC 8605 had already been observed by Thuan and Seitzer (1979) but not detected because the emission does not lie within their covered velocity range. A few profiles shown in Fig. 4 deserve some comments:

UGC 6915 – Belonging to the group of NGC 3995, this galaxy forms a pair with UGC 6920, an Sa 4′ away; however the irregular profile might be due to interaction with a diffuse companion 1′ south.

UGC 7981 – This is a double system, entry 151 in Vorontsov and Vel'yaminov atlas of interacting galaxies (Vorontsov and Vel'yaminov, 1977, hereafter VV), composed by two spirals in close contact that show signs of disruption. The profile shape, a narrow peak on a broader substratum, may be the result of the composite emission from the two galaxies.

UGC 8496 – This is a disrupted multiple system, entry 69 in VV: its optical image consists of three compact condensations surrounded by an extended and irregular gas envelope that may be causing the asymmetric shape of the profile.

UGC 8497 – The optical image of this galaxy shows a compact companion superimposed on its center that might be causing the emission feature close to the left "horn" of the profile.

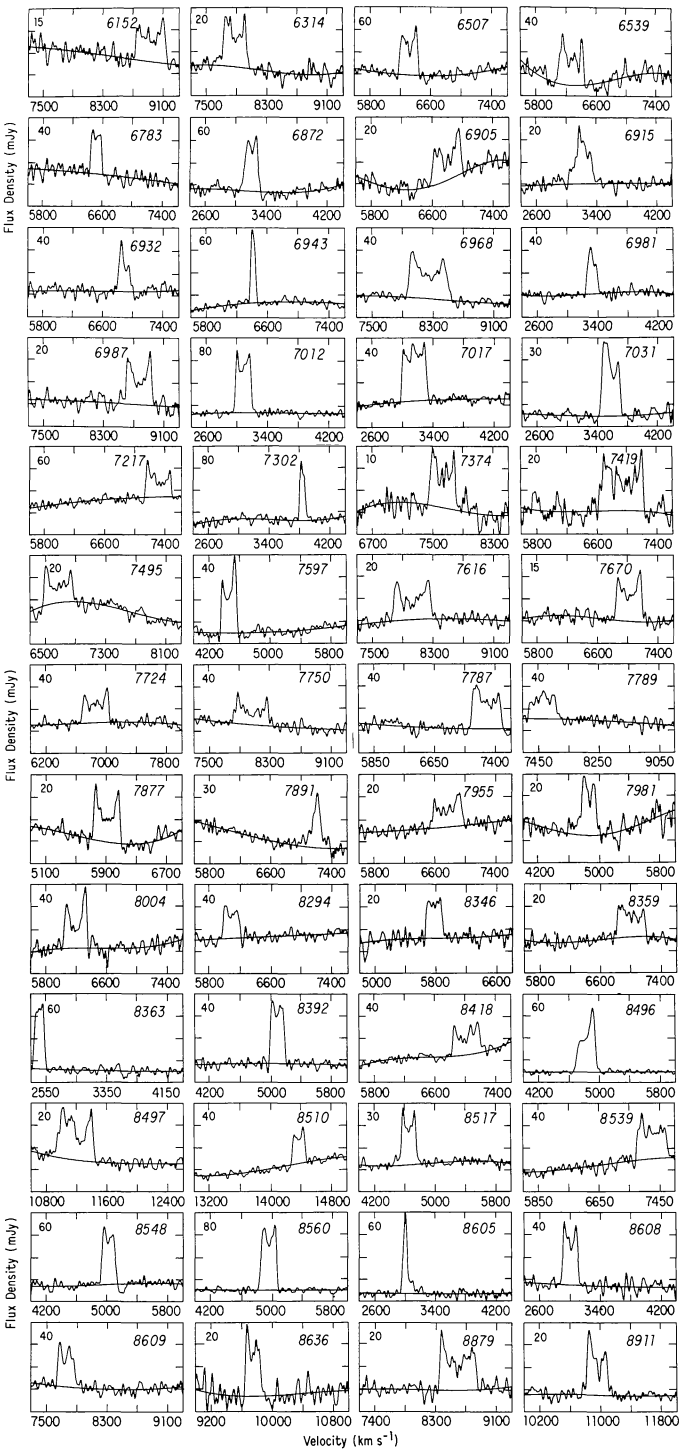

Fig. 4. Twenty-one cm profiles of the detected galaxies: the numbers in the upper left and right corners represent respectively the flux density scale between tick marks and the UGC number. The noiseless polynomial curve superimposed on each profile represents the baseline subtracted before computing the parameters of the line

UGC 8605 – This dwarf spiral forms a pair with the dwarf UGC 8602, located 1.9 west, which may be causing the weak emission on the high velocity side of the profile.

© European Southern Observatory • Provided by the NASA Astrophysics Data System

1984A&A...138...85F

IV. Distribution in velocity

A third spatial dimension is at this stage necessary to investigate whether the filamentary density enhancement that exists in the R.A.-Dec. distribution of galaxies can be the result of projection effects or, instead, it represents a coherent structure in the three dimensional space. Aiming to enlarge the available redshifts sample, we have carried out our 21-cm line observations in the region of the filament. We have then combined our data with all the galaxies redshifts available in the literature within a rectangular region (10^h40^m to 14^h00^m; $+26°$ to $39°$) that contains the most conspicuous part of the filament. The total sample includes 550 objects, it is complete at a limiting magnitude of 14.5 and 80% complete at 15.0. Due to the large number of redshifts available for the area of Coma, within 2° from the cluster center only galaxies brighter than 15.0 have been included in the sample. To visualize the radial distribution of these galaxies, in Fig. 5 we have plotted velocity versus right ascension. The Coma cluster appears as an elongated structure due to the large spread in kinetic energies that the galaxies of its core possess ("Finger of God" effect) but do not appear to be isolated from the rest of the supercluster. An evident characteristic of Fig. 5 is the high degree of non-uniformity shown by the galaxies even in their space distribution: strings of galaxies are connecting several groups defining large and apparently empty regions of space. In the foreground of the Coma supercluster, around 4500 km s^{-1}, a second supercluster is present, as appears also from the data by GT. This structure is connected to the Local supercluster by a long chain of galaxies containing the groups of NGC 4169 ($v \sim 3900$ km s^{-1}, R.A. 12^h30^m), NGC 3995 ($v \sim 3200$ km s^{-1}, R.A. 11^h55^m) and ending in correspondence of the Coma I cloud ($v \sim 800$ km s^{-1}, R.A. 12^h30^m).

The cluster ZW 1319+31, alias ZW 160−7, whose brightest galaxy is erroneously considered to be NGC 5056, requires a more detailed comment. GT have expressed some doubts as to whether the NGC 5056 group belongs to the Coma supercluster: the mean velocity of this group ($v \sim 5500$ km s^{-1}) is in fact substantially lower than the mean velocity of the supercluster. We think that the group of NGC 5056 is indeed in the foreground of the supercluster and not associated with it. However its galaxies appear superimposed on the cluster ZW 160−7 which is on the contrary part of the supercluster: galaxies in the 7000 km s^{-1} range are in fact found inside the contour of ZW 160−7. The indication that the group of NGC 5056 and the cluster ZW 160−7 are two distinct physical associations is in part corroborated by the distribution of the observed redshifts within the contour of ZW 160−7: the objects having velocities around 5000 km s^{-1} seem to be found only in the east side of the cluster, close to NGC 5056, while the galaxies in the 7000 km s^{-1} range appear more uniformly distributed in the cluster. However, we want to stress that the present velocity sample is quite poor and only additional observations could rule out other possibilities.

Although some of these groups and other nearby galaxies appear projected on the filament and contribute to its surface density enhancement, a significant population of galaxies is found around 7000 km s^{-1} for almost three hours of right ascension: 40% of the objects in Fig. 5 lie between 6000 and 8500 km s^{-1}, but if we correct for Malmquist bias and consider only galaxies having an absolute magnitude $M < -19.0$ this number rises to about 55%. Around 13^h45^m the mean velocity of the filament seems to increase probably corresponding to the merging of this structure into the velocity domain of the Hercules supercluster ($v \sim 10{,}000$ km s^{-1}). An histogram of the observed radial velocities,

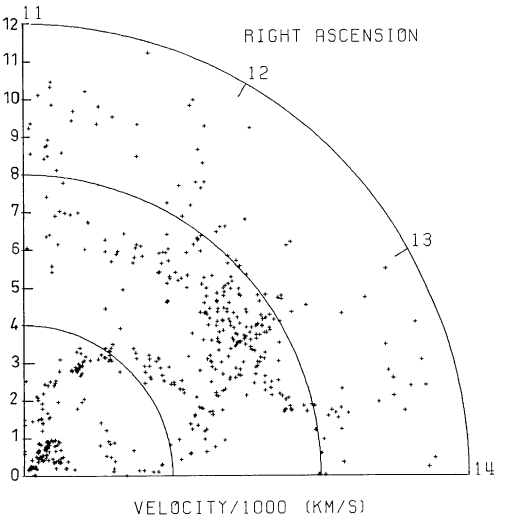

Fig. 5. Cone diagram showing the distribution of the available redshifts within 11^h00^m to 14^h00^m in right ascension and 26° to 39° in declination. Galaxies fainter than 15.0 have been omitted within 2° from the center of Coma

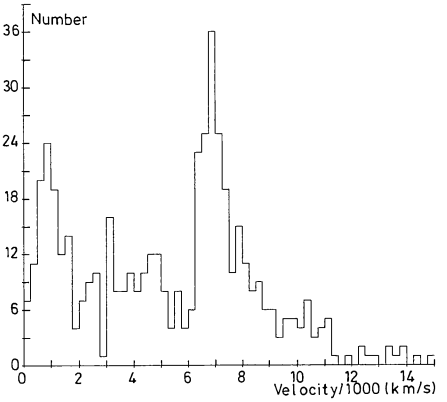

Fig. 6. Histogram of the observed radial velocities: all objects within 2° from the Coma center have been omitted

binned in intervals of 250 km s^{-1}, is shown in Fig. 6: all the galaxies within 2° from the Coma cluster center have been omitted. Between 6000 and 8000 km s^{-1} the mean velocity is 6968 km s^{-1}, with an observed dispersion of 490 km s^{-1}. Secondary peaks in the distribution corresponds to the Local supercluster (Coma I cloud) $v \sim 800$ km s^{-1} and the group of NGC 3995 $v \sim 3200$ km s^{-1}.

Because of the presence of the Coma/A 1367 supercluster in the area of the filament, a legitimate question is whether the galaxies having velocities around 7000 km s^{-1} are found to lie out of the filament's ridge, i.e. in areas associated with the supercluster but not with the filament. To answer this question we have divided the sample into two parts (Fig. 7): galaxies within ±1°.5 from the filament axis (hatched part, containing only 1/3 of the total number of objects) and those which lie outside (white area). Figure 7 shows that there is no substantial difference between the two velocity distributions: if we apply a correction in order to have the same number of objects in the two samples, the galaxies along the filament produce a higher peak around 7000 km s^{-1} than those that lie outside. All this confirms that the filament is a structure

© European Southern Observatory • Provided by the NASA Astrophysics Data System

1984A&A...138...85F

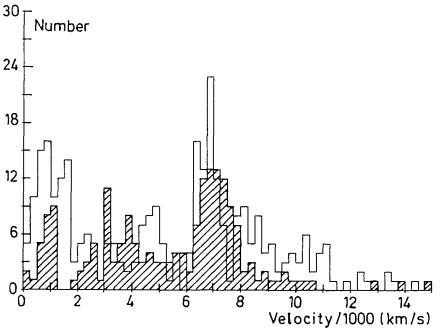

Fig. 7. Histograms of the observed radial velocities shown in Fig. 6 but divided according to their position: hatched part contains galaxies that lie within $\pm 1^{\circ}.5$ from the filament axis, white part contains those that lie outside

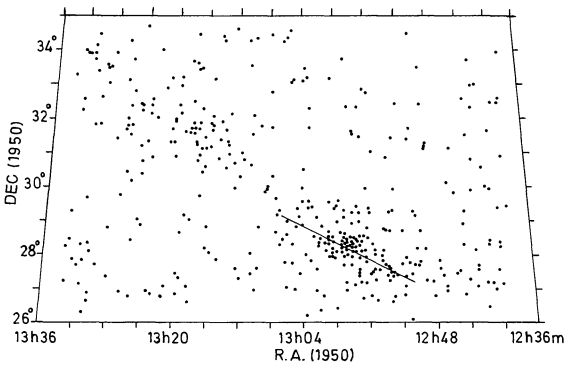

Fig. 8. The area of the filament containing the Coma ($12^{h}57^{m}, 28°$) and ZW 160−7 ($13^{h}20^{m}, 31°$) clusters. The shape of both clusters is elliptical and their major axes are positioned along that of the filament. The solid line shows the orientation of the major axis of Coma (67° with respect to the North-South direction)

embedded in the general area of the supercluster of which it represents a significant density enhancement.

The boundaries of the Coma/A 1367 supercluster, like those of many others, are not well known and for declinations north of Coma they have not been investigated. The fact that even in the regions north of Coma there is a population of galaxies with velocities predominantly around 7000 km s^{-1} is indicative that the supercluster is extending in this area, at least up to 39°–40° of declination.

V. Discussion

a) Cluster orientations

The elongations and orientations of clusters of galaxies in supercluster chains is a primary morphological property of these structures. In the Perseus chain all richest clusters (A 426, A 347, A 262) exhibit a certain degree of ellipticity and their major axes appear to be oriented along the chain (Einasto et al., 1980; Gregory et al., 1981). In the case of the Coma filament this effect is particularly evident for the Coma cluster itself and the cluster ZW 160−7 which appear well oriented along the filament. It has been known for many years that the Coma cluster has an elliptical shape (Abell, 1962) with axial ratio of about 0.55 (Schipper and King, 1978). The position angle of the ellipse is 67°, so that its major axis extends within 12° from the filament's axis, pointing toward the cluster ZW 160−7 which also shows an elongated shape in the same direction. A restricted area of the filament containing the two clusters is shown in Fig. 8 where individual galaxies from the CGCG+UGC sample are plotted. It is also remarkable that extending Coma's major axis toward the south-east for about 20° we find A 1367, the second rich condensation of the supercluster. Even if among the other clusters associated with the filament none seems to exhibit a significant elongation, we think that the observed orientation of Coma and ZW 160−7 is very unlikely to be a coincidence, but instead it is strongly related to the presence of the filament and its origin. For Coma, in fact, the high degree of ellipticity cannot be explained in terms of rotation: the absence of a dynamically significant rotation is well established (Rood et al., 1972; Gregory, 1975).

The fact that neighbouring clusters have a strong statistical tendency to point to each other have been demonstrated by Binggeli (1982). Even if the possibility that clusters elongations and orientations are at least in part the result of tidal distortions cannot be excluded, Binggeli has shown that his results are in good agreement with the adiabatic theory of galaxy and cluster formation (Doroshkevich et al., 1978 and references therein). This theory can be invoked to explain not only the origin of the aspherical shape observed in many clusters of galaxies, but more generally the origin of filamentary structures and their associated "voids". In the adiabatic scenario the dissipative collapse of supercluster material lead to the formation of thin gaseous condensations – so called "pancakes" – from which elongated non-rotating clusters as well as more complex linearly extended features could have subsequently formed: shapes and orientations of clusters would be relics of their origin in highly flattened "pancakes".

A preferential orientation of galaxy position angles in supercluster chains is also likely to exist, although at the moment it is not firmly established. Studying the position angle distribution in the Perseus chain, Gregory et al. (1981) have shown that "the major axis of the supercluster roughly coincides with one peak of the galaxian position angle distribution". For the Coma filament the results of this investigation, carried out using new plates taken with the 48″ Schmidt telescope at Palomar, will be given in a future paper (Fontanelli et al., in preparation). If confirmed, the alignement of galaxies in supercluster chains would provide further support to the adiabatic formation scenario, since it seems difficult to explain such phenomenon with evolutionary effects on a randomly formed and oriented set of objects.

b) Possible connection with the Lynx-Ursa Major and Hercules superclusters

One of the most interesting statements made by the russian cosmologists in the framework of the cell structure of the Universe (see for example Jôeever et al., 1978) is that superclusters are not isolated "islands" but they often appear to be in contact with each other and to have elements in common. As a matter of fact the borders of superclusters are observationally not well defined, fact that seems to indicate no clear separation but rather a mild and continuous passage from one supercluster domain into another. This picture applies also to the Coma filament for which no clear ends seem to exist in the direction of its major axis. In Sect. II we have studied the densest part of the filament within an area that

© European Southern Observatory • Provided by the NASA Astrophysics Data System

1984A&A...138...85F

can be considered with confidence as part of the Coma/A 1367 supercluster. Inspection of Fig. 1, however, indicates that the filament may be extending further. To confirm this visual impression a much larger sample of redshifts than that presently available is needed. A few points, however, can be established at present:

1) There is good agreement between the parameters of the Lynx-Ursa Major filament as described by Giovanelli and Haynes (1982) and those derived in this paper for the Coma filament. In particular one notices with interest that the average widths of the two structures and the slopes of the straight lines fitted to the filament axes (west branch for Coma) coincide: this value is in both cases 1°.7 for the width and 22° for the slope. This triggers the suspicion that the two filaments may constitute a single structure that is seen in the 4500 km s^{-1} range in the Lynx-Ursa Major region and at 7000 km s^{-1} in the Coma area. The computed density contrast is higher for the Lynx-Ursa Major than for the Coma filament (3.7 against 2.7). This however is fully expected, having computed the density of two structures located at a different distance with a magnitude limited sample, which becomes more and more incomplete as the distance increases.

2) In the same way the incompleteness of our sample could lower the surface density of the Coma filament as it merges into the Hercules supercluster. (We have seen an indication of such trend of galaxian velocity in Fig. 5). In this velocity range ($v \sim 10{,}000$–$11{,}000$ km s^{-1}) the incompleteness becomes so severe to miss completely the filamentary enhancement.

In this scenario the unusual geometry of the distribution of galaxies and the presence of long and coherent linear features will play a decisive role to discriminate between competing models of galaxy formation.

VI. Conclusions

We discuss a density enhancement in the surface distribution of galaxies in the Coma/A 1367 supercluster that extends with a filamentary shape for approximately 3.5 h in right ascension in the declination range $+26° \div +39°$. The surface density of galaxies in the filament, which is not altered by patchy galactic absorption, is on average a factor 2.7 higher than in the surrounding areas and shows an average width of about 1°.7. Beside Coma, other Zwicky clusters are embedded in the filament. The redshift distribution shows that, although some nearby objects appear projected on the filament, a significant number of galaxies has velocities around 7000 km s^{-1}, the mean velocity of the Coma supercluster. This indicates that the filament is a coherent structure in the three-dimensional space with a linear dimension of at least 60 Mpc.

An attractive property of this structure which seems to strengthen its nature of coherent unit is the elongation and orientation that two of its clusters, Coma and ZW 160 – 7, possess: their major axes are pointing to each other and are significantly oriented along the filament axis. We suggest that the strong ellipticity of Coma, which is not due to rotation, could be related to its origin within the filament structure in the framework of the adiabatic theory of galaxy formation.

The surface distribution of galaxies seems also to indicate that the filament could be part of a longer feature bridging the Lynx-Ursa Major and the Hercules superclusters: strong morphological and positional similarities are found to exist between the Lynx-Ursa major and the Coma filament. Although in agreement with the available data, the connection between the Hercules and Lynx-Ursa major velocity domains needs to be confirmed with a substantially enlarged redshift sample.

At this stage a better understanding of the morphology and origin of filamentary structures appears as a primary objective for theoretical investigations in order to enlarge our knowledge of the physical processes in the early Universe and of the large scale distribution of matter.

Acknowledgements. This research could not have been done without the generous hospitality and financial support of Cornell University at the Arecibo Observatory and of N.R.A.O. in Charlottesville. I wish to thank Drs. R. Giovanelli and M. P. Haynes for their guidance and assistance at the beginning of this project. I am greatful to C. Balkowski for fruitful suggestions and comments and to G. Vettolani for a copy of his catalog of radial velocities. I have also benefited from conversations with Professor J. H. Oort, P. Chamaraux, and B. A. Williams.

References

Abell, G.: 1961, *Astron. J.* **66**, 607
Abell, G.: 1962, in *Problems of extragalactic research*, ed. G. C. McVittie, Macmillan, New York, p. 213
Binggeli, B.: 1982, *Astron. Astrophys.* **107**, 338
Bridle, A.H., Davis, M.M., Fomalont, E.B., Lequeux, J.: 1972, *Astron. J.* **77**, 405
Burstein, D., Heiles, C.: 1978, *Astrophys. J.* **225**, 40
Chincarini, L., Rood, H.J., Thompson, L.A.: 1981, *Astrophys. J.* **249**, L 47
Doroshkevich, A.G., Saar, E.M., Shandarin, S.F.: 1978, in *The Large Scale Structure of the Universe, IAU Symp.* **79**, eds. M. S. Longair, J. Einasto, p. 423
Dressel, L.L., Condon, J.J.: 1976, *Astrophys. J. Suppl.* **31**, 187
Einasto, J., Joeveer, M., Saar, E.: 1980, *Monthly Notices Roy. Astron. Soc.* **185**, 357
Giovanelli, R., Haynes, M.P.: 1982, *Astron. J.* **87**, 1355, 1982
Gregory, S.: 1975, *Astrophys. J.* **199**, 1
Gregory, S., Thompson, L.A.: 1978, *Astrophys. J.* **222**, 784
Gregory, S., Thompson, L.A., Tift, W.G.: 1981, *Astrophys. J.* **243**, 411
Joeveer, M., Einasto, J., Tago, E.: 1978, *Monthly Notices Roy. Astron. Soc.* **185**, 357
Lucey, J.R., Dickens, R.J., Mithcell, R.J., Dawe, J.A.: 1983, *Monthly Notices Roy. Astron. Soc.* **203**, 545
Nilson, P.: 1973, Uppsala General Catalog of Galaxies, Uppsala Astronomiska Observatoriums Annaler, Vol. 1, Band 6
Rood, H.J., Page, T.L., Kintner, E.C., King, I.R.: 1972, *Astrophys. J.* **175**, 627
Schipper, L., King, I.R.: 1978, *Astrophys. J.* **220**, 798
Shane, C.D., Wirtanen, C.A.: 1967, Publ. Lick Obs., Vol. 22, Part I
Thuan, T.X., Seitzer, P.O.: 1979, *Astrophys. J.* **231**, 327
Vorontsov-Vel'yaminov, B.A.: 1977, *Astron. Astrophys. Suppl.* **28**, 1
Zwicky, F., Herzog, E., Wild, P., Karpowicz, M., Kowal, C.T.: 1961–1968, Catalog of Galaxies and Clusters of Galaxies, Cal. Inst. Tech., Pasadena, Vols. 1–6

© European Southern Observatory • Provided by the NASA Astrophysics Data System